Segmentation Algorithms for Choroidal OCT Images

Lakku Praveen Kumar Reddy

A Thesis Submitted to
Indian Institute of Technology Hyderabad
In Partial Fulfillment of the Requirements for
The Degree of Master of Technology

भारतीय प्रौद्योगिकी संस्थान हैदराबाद
Indian Institute of Technology Hyderabad

Department of Electrical Engineering

June 2016

Declaration

I declare that this written submission represents my ideas in my own words, and where ideas or words of others have been included, I have adequately cited and referenced the original sources. I also declare that I have adhered to all principles of academic honesty and integrity and have not misrepresented or fabricated or falsified any idea/data/fact/source in my submission. I understand that any violation of the above will be a cause for disciplinary action by the Institute and can also evoke penal action from the sources that have thus not been properly cited, or from whom proper permission has not been taken when needed.

(Signature)

Lakku Praveen Kumar Reddy

(Lakku Praveen Kumar Reddy)

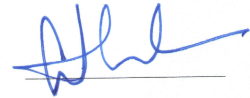EE14MTECH11005

(Roll No.)

Approval Sheet

This Thesis entitled Algorithms for Blood Vessel Segmentation in 2-D Choroidal Scan Images and Objective Performance Evaluation of Such Algorithms by Lakku Praveen Kumar Reddy is approved for the degree of Master of Technology from IIT Hyderabad
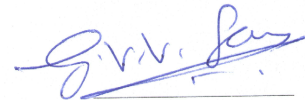
(Dr. Subha Narayan Rath) Examiner
Dept. of Biomedical Engineering
IITH

(Dr. Lakshmi Prasad Natarajan) Examiner
Dept. of Electrical Eng
IITH

(Dr. Sumohana S. Channappayya) Adviser
Dept. of Electrical Eng
IITH

(Dr. G V V Sharma) Chairman
Dept. of Electrical Eng
IITH

Acknowledgements

Abstract

Choroid of the human eye mostly consists of blood vessels, through these vessels it supplies oxygen and nutrition to retina, sclera regions. Blood vessels of choroid are an indication of health of the eye. Opthamologist will observe the structural changes in the choroid through Optiacl Coherence Tomography(OCT) scans. To assist the opthamologist in the diagnosis, we present an automated algorithm for detection of choroidal blood vessels. We are proposing two methods. One method is simple, finding the region of interest and applying Laplacian of Gaussian. In the second method we formulated this segmentation problem as a binary classification problem. Classification is done by estmating the probability density functions of choroidal vessel region and stromal region by using mixture of gaussians.

Contents

Chapter 1

Introduction

Image segmentation is among the most widely studied image processing techniques due to its wide ranging applications.Some of them are locating objects in satellite images , face detection, pedestrian detection, locating tumors in diagnostic images etc. The main goal of image segmentation is changing the representation of image. We can define image segmentation in many ways. Image segmentation is the process of assigning a label to every pixel in an image, pixels having same label will be considerd as one segment. The labeling will be done such that pixels having same label will share certain common properties. The following list is a set of different methods used for image segmentation.

1. Thresholding methods

2. Clustering methods

3. Histogram based methods

4. Edge detection methods

5. Region growing methods

6. Grapg partitioning methods

7. Markov random fields

In this work we are detecting the blood vessels in 2-D choroidal scan images. The choroid is a vascular layer thats to say its made up of blood vessels and capillaries, located between the sclera and retina. It supplies blood and nutrients to the retina and nourishes all of other structure within the eye. The figure 4.2 shows the strucutre of eye.

It also regulates retinal heat assists in the control of intraocular pressure and absorbs excess light, thus avoiding internal reflection. In humans the thickness of the choroid will be 200 μm at
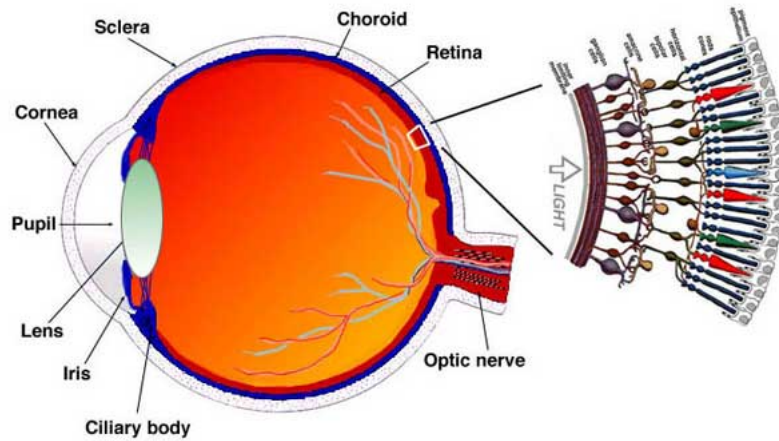
Figure 1.1: strucuture of eye

the time of birth and it eventually decreases to about 80 μm by the age 90. If the choroid cannot supply oxygen and nutrients through the blood to those layers then obviously the eye will begin to suffer the sclera will begin to dry out, become inflamed and form ulcers, whilst the retina will not be able to process the light that it receives into messages for the brain. It is well known that the one set of diseases or ageing changes the structure of the choroidal stroma, particularly vessel thickness and volume. To observe the changes in choroid with disease or ageing optical coherence tomography (OCT) imaging is considered as a useful tool. Sample OCT image is shown in the Figure 1.2.

Figure 1.2: OCT image
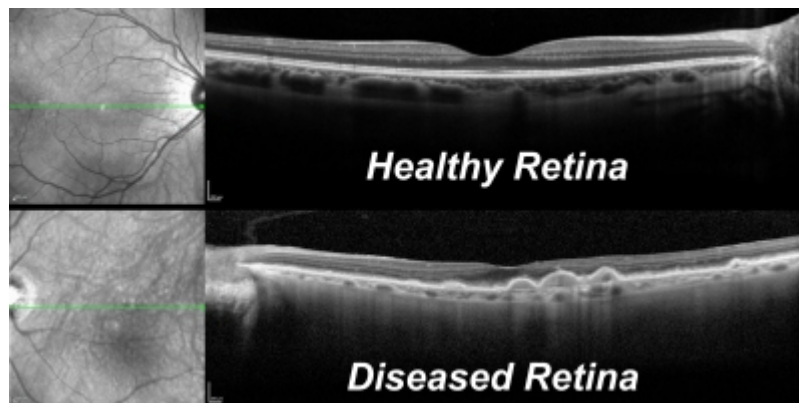
However, presence of speckles, low contrast and high absorption of light makes an OCT image difficult to understand.

we proposed two methods to dectect blood vessels in these OCT images.One method is using the conventional approaches edge setection and thresholding. Other method uses a probabilistic framework. Several reserchers have also proposed different methods to perform the same task.

Whereas little work done in evaluating the performance of these algoritms. Up to now best method to evaluate the performance of segmentation algorithms is subjective evaluation which means expert will observe the outputs of algorithms and rank their performance accordingly.

In the context of biomedical images, subjective evaluation of the segmentation output by an expert is considered the gold standard. While this evaluation strategy is indeed the best in terms of its efficacy, it is very expensive and time consuming given the large volume of clinical data. To address the issue of large data volume, an alternative to subjective assessment is *objective* or *automated* quality assessment of segmentation that is able to mimic expert performance. In this work, we present an objective methodology for the evaluation of image segmentation algorithms that is aimed at reducing the requirement for manual quality assessment by a significant amount. We specifically focus on vessel segmentation algorithms that operate on the choroidal OCT images.

To achieve this goal, we examine the wide gamut of objective segmentation evaluation algorithms and suggest a set of five methods that are in our opinion best suited for the task at hand. The various objective evaluation methods for performance evaluation can broadly be categorized into

1. Supervised evaluation

2. Unsupervised evaluation

In supervised evaluation, the algorithmic output is compared against manually segmented images. As the name suggests, unsupervised evaluation methods do not use any reference results for comparison. In the unsupervised case, performance is evaluated by checking for some desirable properties in the segmented image. The interested reader is referred to Zhang et al. [1] for a survey on unsupervised methods. Our work is focused on supervised evaluation.

Chapter 2

Literature

Many reserchers proposed algorithms to segment the 2D choroidal scan images. Some of them focused on detecting different layers present in the choroid, while others focused on segmenting the choroidal vasculature and measuring the thickness of vessels. Zhang et al. [2] proposed a fully-automated 3D method to segment and visualize the choroidal vasculature in macular scans. Local vascuulature and choriocapillaris equivalent thickness were determined. Their dataset includes scans of 24 normal subjects.

A. Mishra et al. [3] proposed an algorithm to segment individual retinal layers present in retinal OCT imagery. It is a two-step kernel-based optimization scheme. First step is to identify the approximate locations of the individual layers, which are then refined to obtain accurate segmentation results for the individual layers.

Stephanie et al. [4] presents an automatic approach for segmenting retinal layers in Spectral Domain Optical Coherence Tomography images using graph theory and dynamic programming. This method accurately segments eight retinal layer boundaries in normal adult eyes more closely to an expert grader.

M.pircher et al. [5] presents a new method for identifying and segmenting the retinal pigment epithelium (RPE) in polarization sensitive optical coherence tomography (PS-OCT) images of the human retina. Two different segmentation algorithms are presented and discussed: a simpler algorithm based on retardation data, and a more sophisticated algorithm based on local variations of the polarization state calculated from averaged Stokes vector elements.

srinath et al. [6] proposed an algorithm for detection of choroid sclera boundary using SSIM [7] index, detection o vessels using level set method. Mahajan et al. [8] proposed a novel algorithm for the detection of blood vessel contours in 2D-OCT choroidal scan images and finding their area. Due to different sizes of blood vessels present in choroidal region, 3 different detection methods are used.

- Boundary sensitive detection

- Intensity sensitive detection

- Vessel enhancement and detection

Boundary sensitive detection is used for contrast enhancement and it helps in finding closely located blood vessels. Intensity sensitive detection plays a major role in finding small blood vessels, where as vessel enhancement and detection clearly locates all major blood vessels present in choroidal region. Finally all the three methods were combined such that the algorithm detects all kinds of blood vessels.

Several researchers have worked on evaluation of boundary detection algorithms. Some authors explained their results with synthetic images, while others explained with actual medical images. Chalana and Kim [9] worked on cardiac ultrasound images. They evaluated performance of epicardial and endocardial boundaries detection algorithms. They also addressed some of the challenges faced in medical image segmentation evaluation.

Jiang et al. [10] defined distance measures for image segmentation evaluation. They interpreted image as a set O of pixels and segmentation as a clustering of O. This leads to define many distance measures. Zhang et al. [1] did an elaborated survey on unsupervised evaluation methods. They also explained each metric's advantages and disadvantages using some synthetic images.

Dice coefficient is commonly used to evaluate the performance of segmentation algorithms. It is defined in the following way.

$$C = \frac{2|A \cap B|}{|A| + |B|}$$

where A and B can be interpreted as either blood vessels or images. For choroidal images, we cannot use dice coefficient directly due to the following reasons. In most of the choroidal images, the number of blood vessels in reference image and segmented image are not equal so we cannot interpret A and B as blood vessels. If we consider A and B as images, its intersection value will be very high because vessels occupy only 20% area in the image and remaining 80% is same in A and B. Due to this, we get very high correlation values. Similarly, many of the the standard metrics used in evaluating image segmentation techniques are found not suitable for our purpose. So, we present a set of 5 similarity measures which gives the most comprehensive picture of how the choroidal vessel segmentation algorithm performs.

Chapter 3

Algorithm for blood vessel detection using LoG

The automated segmentation of vessels in the choroidal region will assist the opthomoligist in the diagnosis of various eye diseases. We tried to solve this problem using two approaches. One method is using Laplacian of Gaussian operator, second method is using probabilistic frame work. Second method will be discussed in the next section. Main motivation for this method is the algorithms developed upto now are complex methods, they need more computations. We tried a very simple approach. The algorithm consists of mainly 3 steps

1. Denoising

2. Finding the region of interest

3. Detecting blood vessels in the ROI

3.1   Denoising

Noise is inherent in these images due to the acquisition process involved in medical imaging techniques. More often segmentation algorithms include difference operations. we know that these difference operations will increse the noise present in the images. So to avoid this we are first smoothing the image using well known BM3D algorithm by Dabov et al. [11]. In this method similar 2D image fragments(e.g blocks) are grouped to form 3D data arrays. By applying 3D transform on this and shrinkage of the spectrum will lead to removal of noise. Inverse 3D transform will give the denoised output.
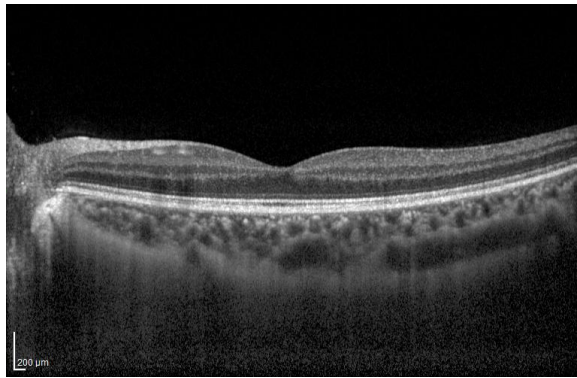
(a) Original noisy image
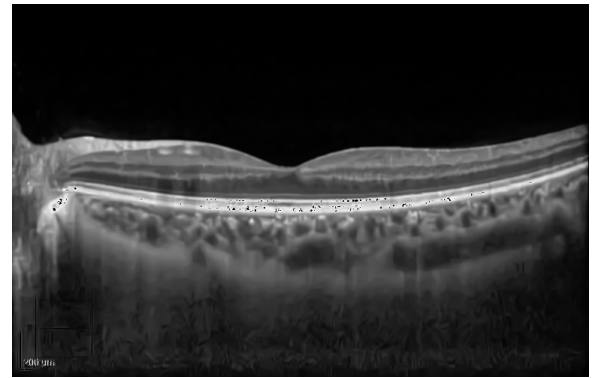
(b) Denoised image

Figure 3.1: BM3D Denoise algorithm output

3.2 Finding the Region of Interest

Finding the ROI consists of two steps. First step is finding the RPE(retinal Pigment Epithalium) layer which lies just above the choroid. Second step is finding the choroid - sclera boundary.

3.2.1 Finding the RPE layer

RPE layer will have high intensity pixels when compared to the remaining region present in the image. By detecting high intensity pixels along each column and by using 4th order polynomial curve fitting RPE layer cab be detected. Choroid region lies below this RPE layer. By removing the all region above RPE we will be left with only choroid and sclera region.
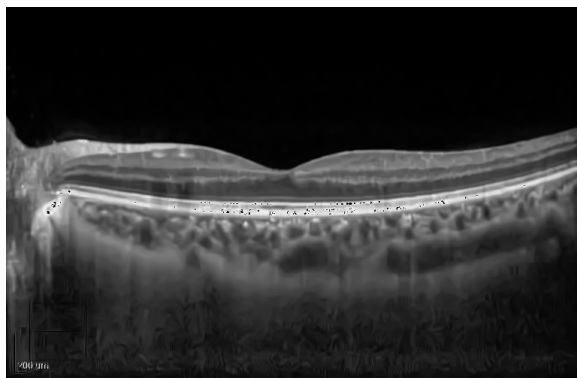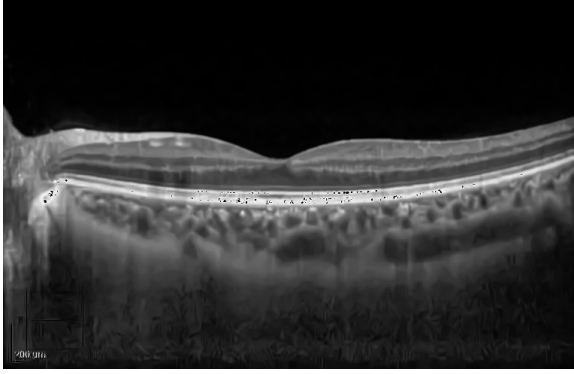

(a) Original denoised image
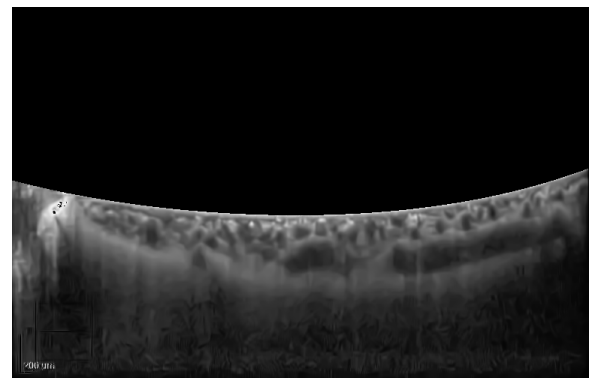
(b) After the removal of retina region

Figure 3.2: Finding the RPE layer

7

3.2.2　Finding choroid-sclera boundary

Firstly gradient along Y- direction is applied. This gradient image is binarised using an empirical threshold value of 1. In this binary Image a band of black pixels will be present just below the choroid region. By using the mid points of this region and using a 4th order polynomial curve fitting we will get a smooth estimate of choroid-sclera boundary. All the region below this curve will be set to an intensity value of zero.


(a) Original denoised image　　　　　　　　　　(b) After the removal of sclera region

Figure 3.3: Image with only Region of Interest

3.3　Detecting blood vessels in ROI

Now the image has only choroid region. We applied Laplacian of Gaussian kernel of size $25 * 25$ with $\sigma = 4$ on the image. In the next step we found all zero crossings in the image. These zero crossings are the boundaries of blood vessels. Some of them may not be closed curves. So we connected the end points of such curves with line segment.

$$LoG(x,y) = \frac{1}{\pi\sigma^4}\left[\frac{x^2+y^2}{2\sigma^2} - 1\right]e^{\frac{-(x^2+y^2)}{2\sigma^2}} \tag{3.1}$$
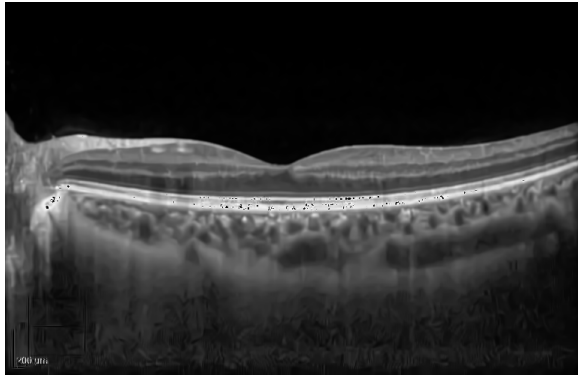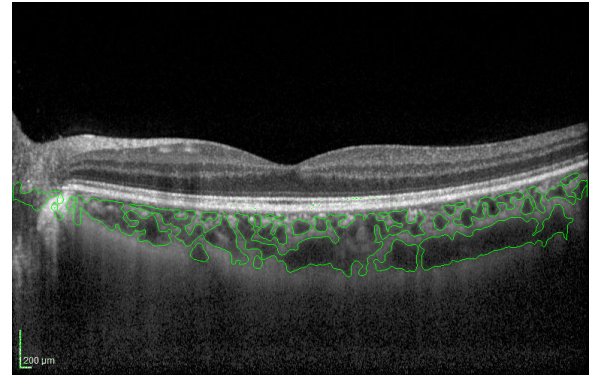
(a) Original denoised image (b) vessels marked image

Figure 3.4: Algorithm output

Chapter 4

Algorithm for blood vessel detection using GMM

Many of the proposed methods are based on conventional approaches like edge detection and threshold, using derivatives information at different stages etc. We tried to solve the image segmentation task using probabilistic approach. Motivation for this approach is " pixel in the output image can be either vessel or not a vessel". So more likely it is a binary classification problem. We have a set of 30 images with corresponding labeled images. We used 24 images for training and 6 images for testing.
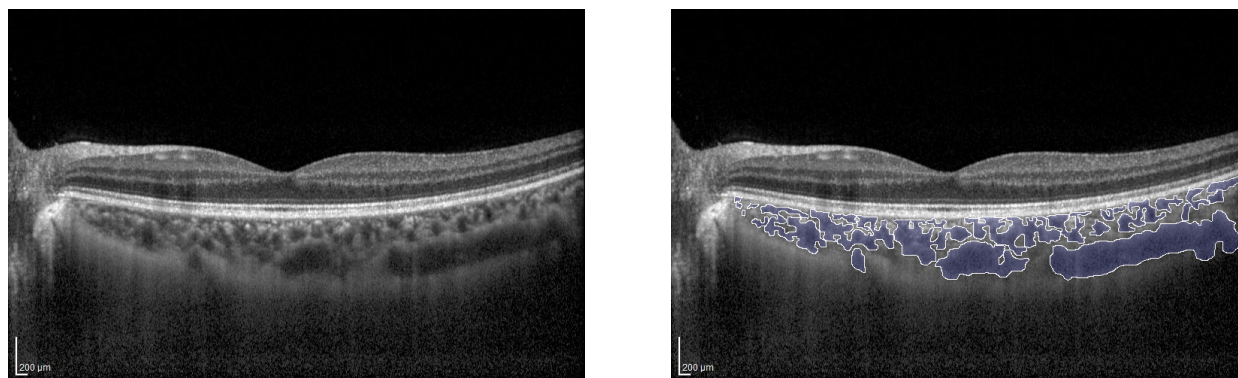
<div align="center">(a) Original image   (b) labeled image</div>

<div align="center">Figure 4.1: Image and its corresponding labeled image</div>

For training data, if we take pixel by pixel values it will be of no use due to the presence of same intenisty values in both choroidal and sclera region. So we have taken pixel and its 8 neighbourhood pixels (left-2, right-2, up-2, down-2).
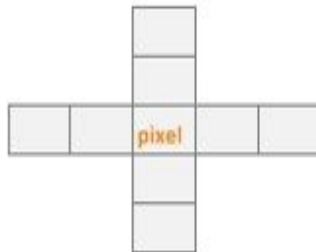
Figure 4.2: 8-neighbours

For this 9 dimensional data we will take the center pixel label information for training. Same procedure is repeated for all training images. Now we will separate the data corresponding to label-1(vessel) and label-0(non vessel). Now we have data for both the label-1 region and label-0 region. We estimated the probability density functions for this two labels by using mixture of Gaussians.

$$p(f/c_1) = \sum_{i=1}^{5} w_i \mathcal{N}(\mu_i, \Sigma_i) \tag{4.1}$$

$$p(f/c_2) = \sum_{i=1}^{5} w_i \mathcal{N}(\mu_i, \Sigma_i) \tag{4.2}$$

$$\tag{4.3}$$

We are using a mixture of 5 gaussians. c_1 corresponds to label-1, c_2 correponds to label-0. The parameters of gaussian mixtures are estimated using EM(Expectation-Maximisation) algorithm. General EM algorithm will have the follwoing steps.

4.1   EM algorithm

Consider we have a dataset of n observations $x_1, x_2, x_3, ..., x_n$ and we wish to model this data using gauusian mixtures. We will assume all data points are drawn independently from the distribution. The log of the likelyhood function is given by

$$\ln P\left(X/\pi, \mu, \Sigma\right) = \sum_{n=1}^{N} \ln \left\{ \sum_{k=1}^{K} \pi_k \mathcal{N}\left(X/\mu_k, \Sigma_k\right) \right\} \tag{4.4}$$

Goal is to maximise this cost function w.r.t the parameters μ_k, Σ_k, π_k. After finding the derivative of the cost function w.r.t these parameters and making it to zero, and some simplification, we wil end up with the follwing steps. First intialise the parameters μ_k, Σ_k

E-step

Evaluate the responsibilities using current parameter values.

$$\gamma\left(\mathcal{Z}_{nk}\right) = \frac{\pi_k \mathcal{N}\left(x_n/\mu_k, \Sigma_k\right)}{\sum_{j=1}^{K} \pi_j \mathcal{N}\left(x_n/\mu_j, \Sigma_j\right)} \tag{4.5}$$

M-step

Re-estimate the parameters using current responsibilities.

$$\mu_k^{new} = \frac{1}{N_k} \sum_{n=1}^{N} \gamma\left(\mathcal{Z}_{nk}\right) x_n$$

$$\Sigma_k^{new} = \frac{1}{N_k} \sum_{n=1}^{N} \gamma\left(\mathcal{Z}_{nk}\right)\left(x_n - \mu_k^{new}\right)\left(x_n - \mu_k^{new}\right)^T$$

$$\pi_k^{new} = \frac{N_k}{N}$$

where

$$N_k = \sum_{n=1}^{N} \gamma\left(\mathcal{Z}_{nk}\right) \tag{4.6}$$

Evaluate the log likelihood

$$\ln P\left(X/\pi, \mu, \Sigma\right) = \sum_{n=1}^{N} \ln \left\{ \sum_{k=1}^{K} \pi_k \mathcal{N}\left(X/\mu_k, \Sigma_k\right) \right\} \tag{4.7}$$

and check for convergence of either the parameters or the log likelihood. If the convergence criterion is not satisfied return to E-step.

4.2   Classification criteria

All the parameters are estimated by using EM algorithm. After estimation of the parameters we have to do the classification (in this framework image segmentation). From the test image we will take pixel and its 8-neighbours. We will substitute these 9 dimensional data in both the pdfs. If lable-1 pdf gives high value than label-0 then pixel is treated as label-1 i.e blood vessel otherwise treated as label-0. This is explained in the following equations.
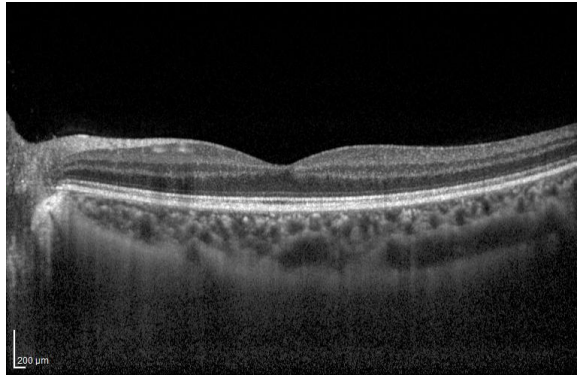
We are assuming a pixel can be vessel or non vessel with equal probability.
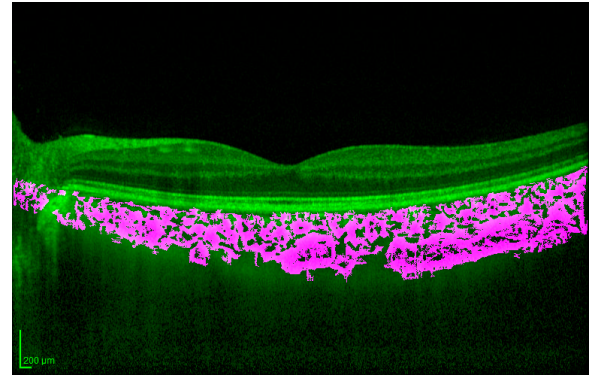
$$P(c_1) = P(c_2)$$

By assuming equal probabilities

$$P(c_1/f) \propto P(f/c_1)$$

If $P(c_1/f) \geq P(c_2/f)$ then output label is $'1'$ i.e blood vessel
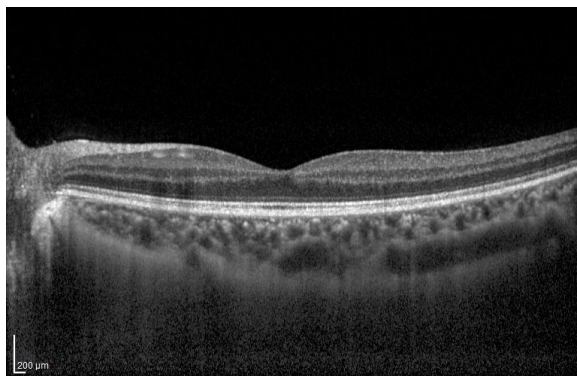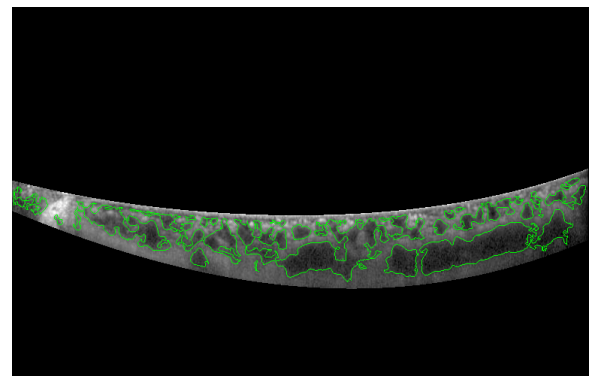

(a) Original image

(b) Output of GMM

Figure 4.3: pink-represents the blood vessel in the output image

GMM output and Laplacian of Gaussian output are logical 'AND'ed and some morphological operations are done to get the final output.

(a) Original image

(b) Output of GMM+LoG

Figure 4.4: final output

13

Chapter 5

Objective Performance Evaluation of Blood Vessel Segmentation Algorithms

Several researchers have proposed different algorithms to detect blood vessels in choroidal scan image, but there is no objective evaluation criteria to evaluate the performance of these algorithms. Here we suggest a set of 5 measures that can be used to evaluate the performance of algorithms objectively. First of all, we binarized algorithm results and manually segmented images such that marked blood vessels appear as white regions and remaining background as black. Reference image and its binarized version are shown in Fig. 5.1a and Fig. 5.1b. Algorithm result and its binarized version are shown in Fig. 5.1c and Fig. 5.1d. In the rest of this document, manually segmented image (ground truth) is labelled as $\mathbf{G}$, as shown in Fig. 5.1b and binarized algorithm result is labelled as $\mathbf{A}$, as shown in Fig. 5.1d.

5.1   Similarity Measure 1

In Sec. 2, we mentioned that Dice coefficient gives high correlation value due to matching of background pixels. To overcome this drawback instead of using matching area, we are taking mismatching area into account. Mismatching area can be calculated using XOR operation. In binary images, the white pixels have a value 1 and black pixels have value 0. The XOR operation returns a HIGH(1) output when both the inputs are different whereas it gives LOW(0) output when both the inputs are similar.
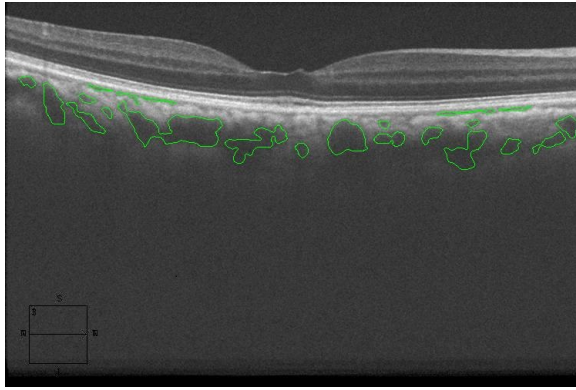
$$\text{Mismatch area} = \text{XOR}(\mathbf{A},\mathbf{G})$$
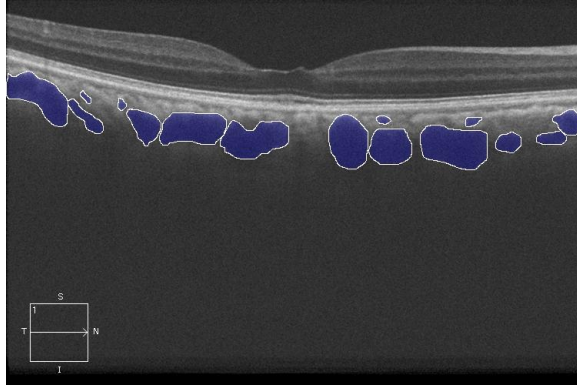
(a) Reference Image.
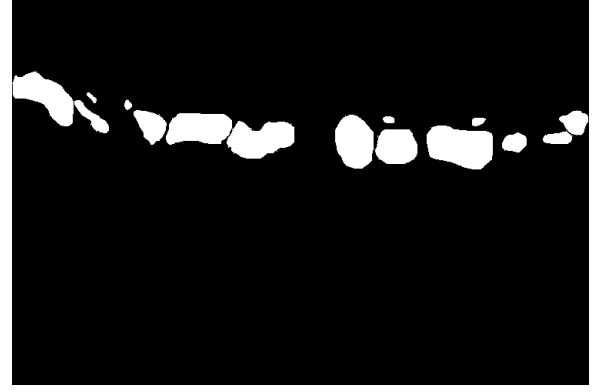
(b) Binarized version of reference image.

(c) Algorithm result

(d) Binarized version of algorithm result

Figure 5.1: Binarization of reference & algorithm result images

Correlation measure is defined as

$$C(\mathbf{A},\mathbf{G}) = 1 - \frac{\text{Mismatch area}}{\text{Total area of blood vessels in } \mathbf{A}\&\mathbf{G}} \qquad (5.1)$$

The algorithm result **A** and the Ground truth image **G** are shown in Fig. 5.2a and Fig. 5.2b. The result of XOR operation between **A** and **G** is shown in Fig. 5.2c. The advantages of using XOR-operation based similarity measure are its simple & intuitive definition and less computation time.

5.2 Similarity Measure 2

Even though the XOR operation based similarity measure is simple and computationally efficient, one major drawback of this measure is that it can't detect over segmentation. For example, if one blood vessel in ground truth image is detected as three blood vessels in algorithm result, still the

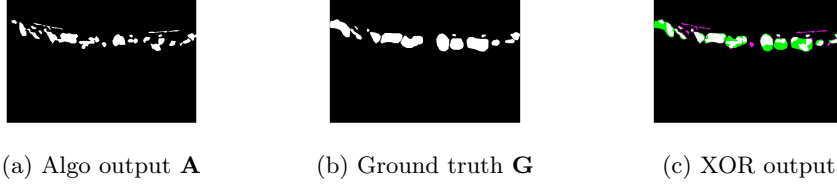(a) Algo output **A**   (b) Ground truth **G**   (c) XOR output

Figure 5.2: Similarity Measure 1 Results
In Fig. 5.2c White - Matching area ; Pink, Green-Mismatch area
Result recorded = Pink + Green area

XOR based similarity measure will give a high correlation value. To overcome this drawback of ignorance of over segmentation, we are using *Similarity Measure 2*. In this measure also, we first found the mismatch area and then calculated the correlation measure. But to tackle the problem of over segmentation, we considered 3 different cases. The over segmentation issue is addressed in the third case.
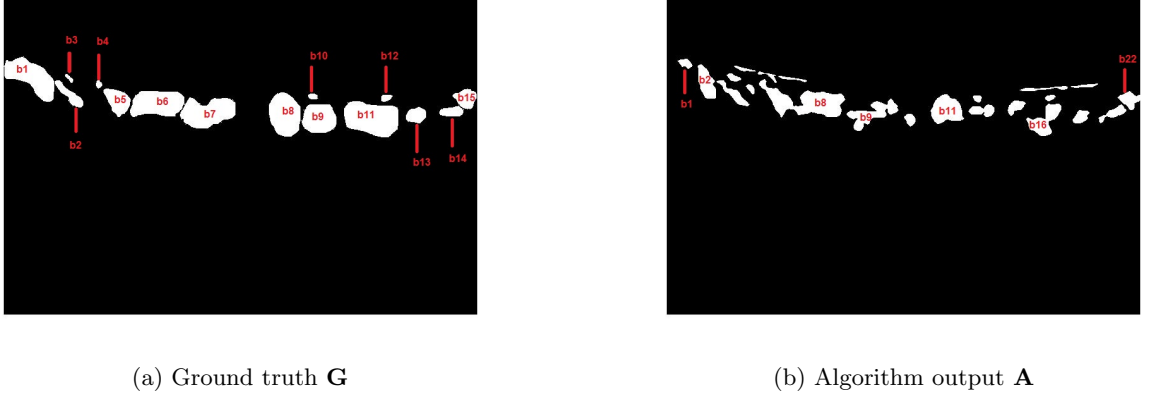

(a) Ground truth **G**   (b) Algorithm output **A**

Figure 5.3: The motivation for our work: Comparing automated output with the "ground truth"

Consider reference image $\mathbf{G} = \{b_1^1, b_1^2, b_1^3, b_1^4, \ldots, b_1^m\}$ and segmented image $\mathbf{A} = \{b_2^1, b_2^2, b_2^3, b_2^4, \ldots, b_2^n\}$, where m and n are the total number of blood vessels in $\mathbf{G}$ and $\mathbf{A}$ respectively. $b_1^1, b_1^2, b_1^3, b_1^4, \ldots, b_1^m$ represents blood vessel regions corresponding to reference image $\mathbf{G}$ as shown in Fig. 5.3a and $b_2^1, b_2^2, b_2^3, b_2^4, \ldots, b_2^n$ represents blood vessel regions corresponding to algorithm result image $\mathbf{A}$ as shown in Fig. 5.3b. We will consider only one blood vessel from $\mathbf{G}$ each time and the overlapping area with each blood vessel that corresponds to $\mathbf{A}$ is calculated. There are three possibilities:

- No blood vessel corresponding to $\mathbf{A}$ is overlapped by the selected blood vessel of $\mathbf{G}$. Then distance is calculated as

$$D_{b_1^1} = \text{Area}(b_1^1)$$

  i.e. the area of the selected blood vessel of $\mathbf{G}$. Consider the case where we have taken one

16

blood vessel from $\mathbf{A}$ (instead of $\mathbf{G}$) as shown in the Fig. 5.4a. Its overlap area w.r.t $\mathbf{G}$ is shown in Fig. 5.4b. In superimposed image, white area represents overlap area. You can observe that there is no white area in Fig. 5.4b.

- Only one blood vessel corresponding to $\mathbf{A}$ is overlapped by the selected blood vessel. Then distance is calculated as

$$D_{b_1^1} = \text{Area}(b_1^1) - \text{Overlap area}$$

This case is explained in figures 5.5a and 5.5b. One blood vessel is taken from $\mathbf{G}$ is shown in the Fig. 5.5a and its overlap w.r.t $\mathbf{A}$ is shown in the Fig. 5.5b.

- If more than one blood vessel corresponding to $\mathbf{A}$ is overlapped by the selected blood vessel of $\mathbf{G}$. We addressed the problem of over segmentation by taking overlapping area of all blood vessels except the area of the blood vessel which gives maximum overlap. Then distance is calculated as

$$D_{b_1^1} = \text{Non-maximal overlap area}$$

The selected blood vessel is shown in the Fig. 5.6a. The superimposed with $\mathbf{A}$ is shown in the Fig. 5.6b.

Same procedure is repeated for all blood vessels. Overall distance from $\mathbf{G}$ to $\mathbf{A}$ is calculated as follows

$$D(\mathbf{G}, \mathbf{A}) = D_{b_1^1} + D_{b_1^2} + \cdots + D_{b_1^m}$$

Similarly D($\mathbf{A}$,$\mathbf{G}$) is calculated as follows

$$D(\mathbf{A}, \mathbf{G}) = D_{b_2^1} + D_{b_2^2} + \cdots + D_{b_2^n}$$

Overall correlation measure between $\mathbf{A}$ and $\mathbf{G}$ is evaluated as

$$C(\mathbf{A}, \mathbf{G}) = 1 - \frac{D(\mathbf{G}, \mathbf{A}) + D(\mathbf{A}, \mathbf{G})}{\text{Total area of blood vessels in } \mathbf{A}\&\mathbf{G}} \tag{5.2}$$

The reasons for taking distance in both directions i.e. $D(\mathbf{A},\mathbf{G})$ & $D(\mathbf{A},\mathbf{G})$ are many. Consider the case where instead of detecting actual blood vessels, the algorithm returns a white rectangular

region as detected blood vessels, as shown in Fig. **??**. In this case $D(\mathbf{G}, \mathbf{A}) = 0$ which means distance between $\mathbf{A}$, $\mathbf{G}$ is zero, it indicates perfect correlation. But this interpretation is absolutely wrong. Whereas $D(\mathbf{A}, \mathbf{G}) \approx$ Area of G. By combining both $D(\mathbf{A,G})$ and $D(\mathbf{A,G})$ total correlation value will get reduced to approximately 0.5. This is the main advantage of calculating both $D(\mathbf{A,G})$ and $D(\mathbf{A,G})$.

If we consider only $D(\mathbf{G}, \mathbf{A})$ it can handle only false negatives and it will not take false positives into account. Similarly $D(\mathbf{A}, \mathbf{G})$ can handle only false positives but not false negatives. By combining both $D(\mathbf{A,G})$ and $D(\mathbf{A,G})$ the similarity measure is able to consider both false positives and false negatives. False positive means vessel present in $\mathbf{A}$ but not in $\mathbf{G}$. False negative means vessel present in $\mathbf{G}$ but not in $\mathbf{A}$.
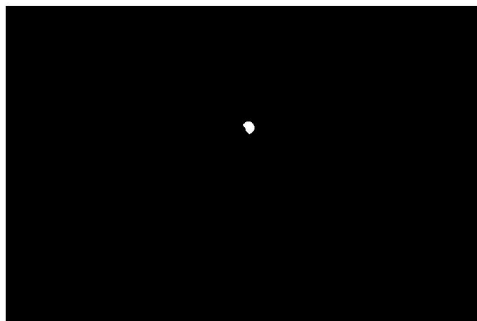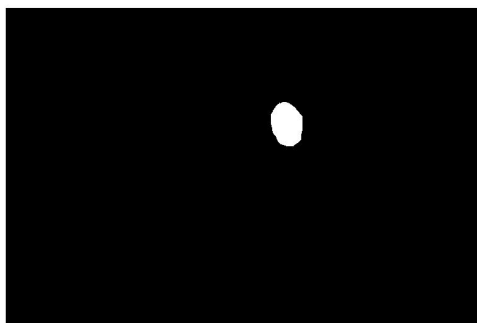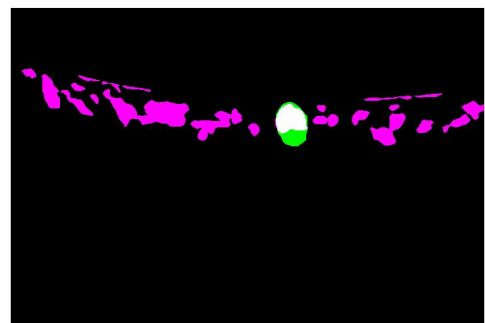

(a) Selected blood vessel
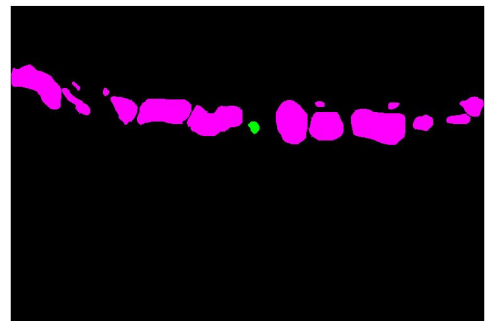
(b) Superimposed image

Figure 5.4: Similarity Measure 2 Case-I : (Pink - Ground truth , Green - Selected blood vessel from algorithm result, white - overlap) Result showing no-overlap
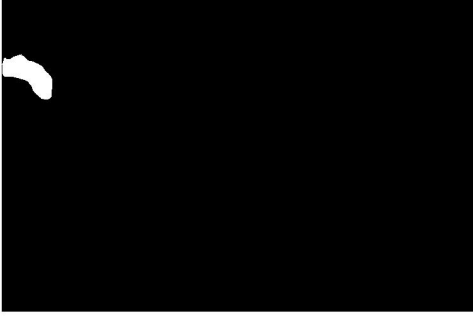In Fig. 5.4b Result recorded = Green area

(a) Selected blood vessel

(b) Superimposed image

Figure 5.5: Similarity Measure 2 Case-II : (White - Overlap area of $\mathbf{A}$ and $\mathbf{G}$, Pink - Non-Overlapping Algorithm result, Green - Non-overlapping ground truth area) Results for one blood vessel over-lapping
In Fig. 5.5b Result recoded = Green area

18

(a) Selected blood vessel   (b) Superimposed image

Figure 5.6: Similarity Measure 2 Case-III : (White - Overlapping area of **A** and **G**, Pink - Non-Overlapping Algorithm Result, Green - Non-overlapping ground truth area) Results for multiple blood vessel overlapping

In Fig. 5.6b Result Recorded = Smaller white region area among two regions

5.3   Similarity Measure 3

The third correlation measure is similar to the second correlation measure in terms of cases, but the key difference is that we used mismatch area in the second measure whereas in the third similarity measure we are using the maximum overlapping area. In the third correlation measure also, only one blood vessel from **G** is considered in each step and overlapping area w.r.t all blood vessels corresponding to **A** are calculated.

$$D_{b_1^1} = \text{Max overlap area}$$

Similarly $D_{b_1^2}, D_{b_1^3}, \cdots, D_{b_1^m}$ are calculated. After that D_{b_1}, D_{b_2} are calculated as

$$D_{b_1} = D_{b_1^1} + D_{b_1^2} + \cdots + D_{b_1^m}$$

$$D_{b_2} = D_{b_2^1} + D_{b_2^2} + \cdots + D_{b_2^n}$$

Finally the correlation measure is defined as follows

$$C(\mathbf{A},\mathbf{G}) = \frac{D_{b_1} + D_{b_2}}{\text{Total area of blood vessels in } \mathbf{A}\&\mathbf{G}} \tag{5.3}$$

If no blood vessel is overlapped then $D_{b_1^k} = 0$ as is shown in the figures 5.7a and 5.7b. The situation where only one blood vessel is overlapped is explained in figures 5.8a and 5.8b. In case where more than one blood vessel overlaps, we consider only the area of the blood vessel which gives maximum overlap and neglect other overlapping blood vessels, as shown in figures 5.9a and 5.9b.
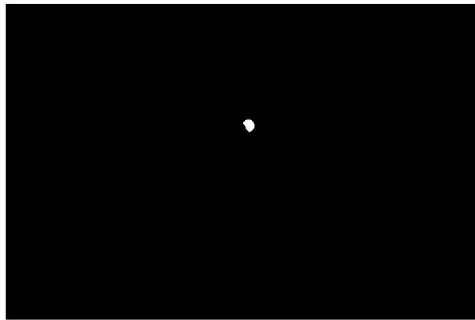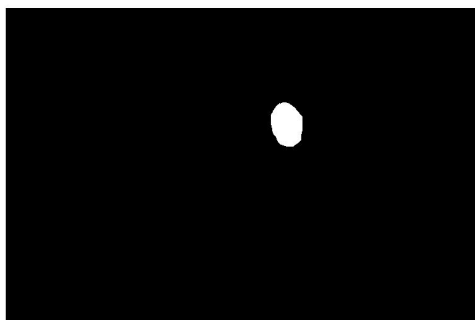
(a) Selected blood vessel
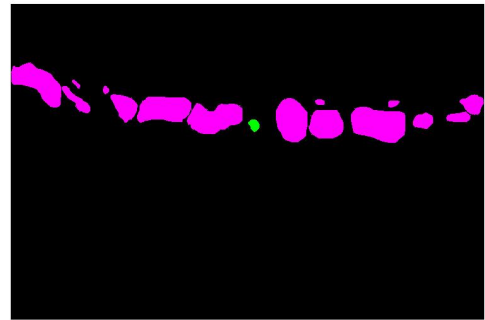
(b) Superimposed image

Figure 5.7: Similarity Measure 3 Case-I : (White - Overlapping area of **A** ,**G**,Pink - Ground truth, Green - Selected blood vessel from algorithm result) Result showing no-overlap
Recorded result = 0

(a) Selected blood vessel
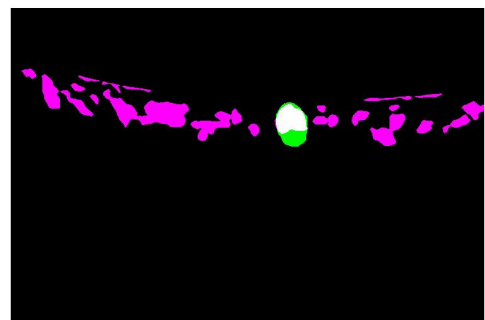
(b) Superimposed image

Figure 5.8: Similarity Measure 3 Case-II : (White - Overlapping area of **A** ,**G**, Pink - Non-Overlapping Algorithm result, Green - Non-overlapping ground truth area) Results for one blood vessel over-lapping
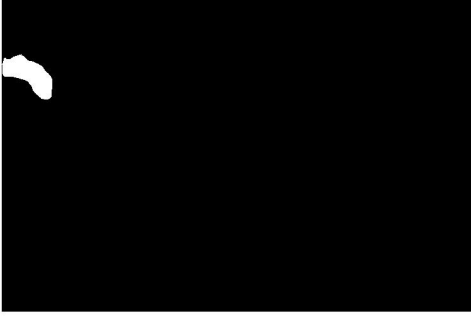Recorded Result = White area

(a) Selected blood vessel   (b) Superimposed image

Figure 5.9: Similarity Measure 2 Case-III : (White - Overlapping area of **A** ,**G**,Pink - Non-Overlapping Algorithm Result,Green - Non-overlapping area) Results for multiple blood vessel overlapping
Recorded result = Area corresponding to larger white region

5.4   Similarity Measure 4a and 4b

In the above measures we used either overlapping area or mismatch area to find correlation. Where as in this similarity measures we are using a different approach. These measures are based on the labels of all possible pairs of pixels.

First we found rectangular region in the images to which we are going to apply the algorithm(to calculate performance measure). In the images **A** and **G** we searched for first white pixel locations. The minimum row number of these two locations was labeled as F_r. Similarly last location of white pixels in **A** and **G** is found. Maximum row number of these two pixel locations is labeled as L_r. Our region of interest is rectangular region bounded by F_r, L_r. Total number of pixels in this region is

$$p = (L_r - F_r + 1) * (no\ of\ columns\ in\ A)$$

We will consider all pair of pixels in image. For example $[\{(p,1),(p,2)\},\{(p,1),(p,3)\},\{(p,1),(p,4)\},\ldots$
$\{(p,1),(p+1,1)\},\{(p,1),(p+1,2)\},\{(p,1),(p+1,3)\},\ldots$
$\{(p,2),(p,3)\},\{(p,2),(p,4)\},\{(p,2),(p,5)\},\ldots]$. Total number of possible pairs is $\binom{p}{2}$.

Labeling is done for the images **A** and **G** such that vessels will be labeled with non zero numbers and background is labeled as zero. Let us assume p_1, p_2 are pixel locations. Consider p_1, p_2 are labeled as g_1, g_2 in image **G** and a_1, a_2 in image **A**. Consider a pair of pixels p_1, p_2 it must belongs to one of the following category.

1. $a_1 = a_2$ and $g_1 = g_2$ (Total number of such pairs are denoted by N_{11}). This case is explained

in figures 5.10a and 5.10b. Red color dots represents pixel locations.

2. $a_1 \neq a_2$ and $g_1 \neq g_2$ (Total such pairs equal to N_{00}). The figures shown in 5.11a and 5.11b pictorially represents this scenario.

3. $a_1 = a_2$ and $g_1 \neq g_2$ (N_{01}). Corresponding images are shown in figures 5.12a and 5.12b.

4. $a_1 \neq a_2$ and $g_1 = g_2$ (N_{10}). Figures 5.13a and 5.13b represents this case.

Obviously $N_{11} + N_{00} + N_{01} + N_{10} = \binom{p}{2}$. By using $N_{11}, N_{00}, N_{01}, N_{10}$ we can define some correlation measures. Among them N_{11} represents some kind of matching percentage. By using this fact, correlation measures are defined in the following way.

$$C(\mathbf{A},\mathbf{G}) \quad = \quad \frac{N_{11} + N_{00}}{\binom{p}{2}} \tag{5.4}$$

$$C(\mathbf{A},\mathbf{G}) \quad = \quad \frac{N_{11}}{N_{11} + N_{10} + N_{01}} \tag{5.5}$$

(a) [Pixels(Red Dots) belonging to same label in algorithm result]
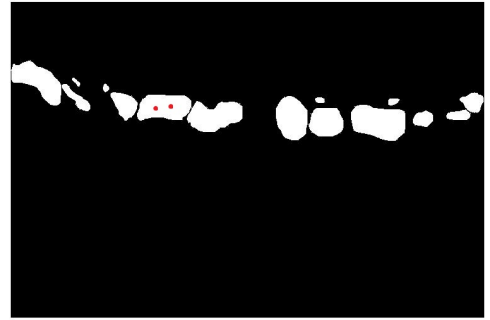
(b) [Pixels(Red Dots) belonging to same label in ground truth result]

Figure 5.10: Similarity Measure 4a & 4b Case-1 : $a_1 = a_2$ and $g_1 = g_2$

(a) [Pixels(Red Dots) not belonging to same label in algorithm result]

(b) [Pixels(Red Dots) not belonging to same label in ground truth result]

Figure 5.11: Similarity Measure 4a & 4b Case-2 : $a_1 \neq a_2$ and $g_1 \neq g_2$

(a) [Pixels(Red Dots) belonging to same label in algorithm result]

(b) [[Pixels(Red Dots) not belonging to same label in ground truth result]

Figure 5.12: Similarity Measure 4a & 4b Case-3 : $a_1 = a_2$ and $g_1 \neq g_2$

(a) [Pixels(Red Dots) not belonging to same label in algorithm result]
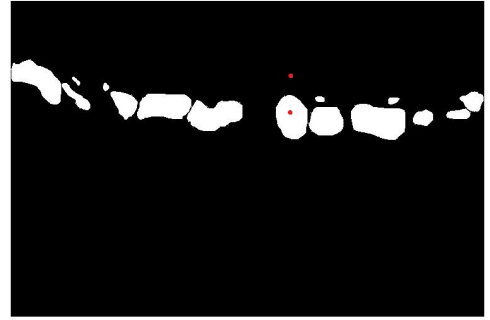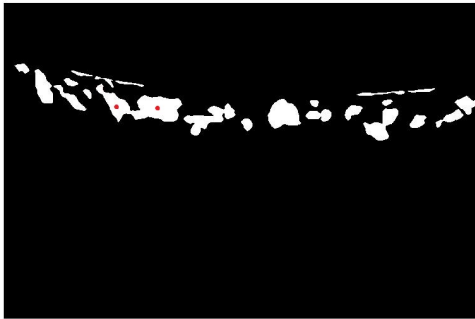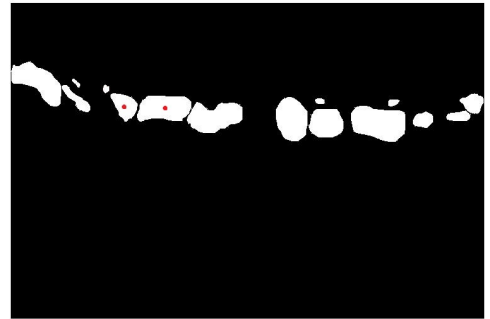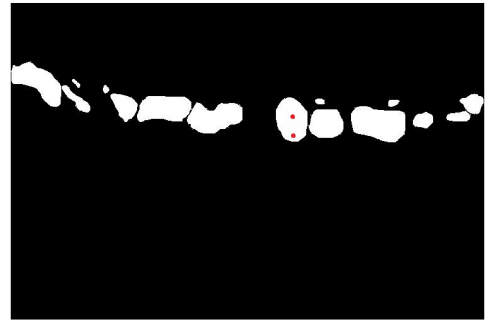

(b) [Pixels(Red Dots) belonging to same label in ground truth result]

Figure 5.13: Similarity Measure 4a & 4b Case-4 : $a_1 \neq a_2$ and $g_1 = g_2$

Chapter 6

Results and Discussions:

Performance of binary classifier will be evaluated on the basis of its classification accuracy.The following table 6.1 shows the classification accuracy of GMM classifier.

Image no	% of accuracy
1	0.8025
2	0.8570
3	0.7996
4	0.8242
5	0.7537
6	0.7696

Table 6.1: Table to show the classification accuracy of GMM model

We compared the results of algorithm proposed by Mahajan et al. [8] with the proposed algorithms. For the ease of comparison first we binarised the outputs such that vessels will become white(binary image) and remaining image black. By using the following measure we compared the algorithms.

$$C(A,G) = 1 - \frac{mismatch\,area\,of\,A,G}{total\,area\,of\,blood\,vessels\,in\,A,G}$$

Where A denotes the binarised version of algorithm output, G denotes the binarised version of Ground truth(labeled) image. Mismatch area is calculated by doing logical "XOR" operation between A,G. The following table 6.2 shows the results of comparison

Image no	Mahajan	LoG	GMM	GMM+LoG
1	0.7067	0.6784	0.5929	0.6893
2	0.7072	0.7611	0.6466	0.7517
3	0.6376	0.7082	0.6299	0.7161
4	0.6302	0.7542	0.6763	0.7518
5	0.7076	0.6672	0.5866	0.6915
6	0.6954	0.7218	0.6091	0.7117

Table 6.2: Comparison of different algorithms

Chapter 7

Conclusion and future work

First method using Laplacian of Gaussian operator is simple, when compared with the previous algorithms and it also giving silghtly better results. Second method using Gaussian Mixture Model is a different framework. Classification accuracy of the model is reasonably well. We used intensity values as features. By using good features and model results can be improved.

References

[1] H. Zhang, J. E. Fritts, and S. A. Goldman. Image segmentation evaluation: A survey of unsupervised methods. *computer vision and image understanding* 110, (2008) 260–280.

[2] L. Zhang, K. Lee, M. Niemeijer, R. F. Mullins, M. Sonka, and M. D. Abramoff. Automated Segmentation of the Choroid from Clinical SD-OCTAutomated Segmentation of Choroid from SD-OCT. *Investigative ophthalmology & visual science* 53, (2012) 7510–7519.

[3] A. Mishra, A. Wong, K. Bizheva, and D. A. Clausi. Intra-retinal layer segmentation in optical coherence tomography images. *Optics express* 17, (2009) 23,719–23,728.

[4] S. J. Chiu, X. T. Li, P. Nicholas, C. A. Toth, J. A. Izatt, and S. Farsiu. Automatic segmentation of seven retinal layers in SDOCT images congruent with expert manual segmentation. *Optics express* 18, (2010) 19,413–19,428.

[5] E. Götzinger, M. Pircher, W. Geitzenauer, C. Ahlers, B. Baumann, S. Michels, U. Schmidt-Erfurth, and C. K. Hitzenberger. Retinal pigment epithelium segmentation by polarization sensitive optical coherence tomography. *Optics express* 16, (2008) 16,410–16,422.

[6] N. Srinath, A. Patil, V. K. Kumar, S. Jana, J. Chhablani, and A. Richhariya. Automated detection of choroid boundary and vessels in optical coherence tomography images. In 2014 36th Annual International Conference of the IEEE Engineering in Medicine and Biology Society. IEEE, 2014 166–169.

[7] Z. Wang and A. C. Bovik. Mean squared error: love it or leave it? A new look at signal fidelity measures. *Signal Processing Magazine, IEEE* 26, (2009) 98–117.

[8] N. R. Mahajan, R. C. R. Donapati, S. S. Channappayya, S. Vanjari, A. Richhariya, and J. Chhablani. An automated algorithm for blood vessel count and area measurement in 2-D choroidal scan images. In Engineering in Medicine and Biology Society (EMBC), 2013 35th Annual International Conference of the IEEE. IEEE, 2013 3355–3358.

[9] V. Chalana and Y. Kim. A methodology for evaluation of boundary detection algorithms on medical images. *Medical Imaging, IEEE Transactions on* 16, (1997) 642–652.

[10] X. Jiang, C. Marti, C. Irniger, and H. Bunke. Distance measures for image segmentation evaluation. *EURASIP Journal on Applied Signal Processing* 2006, (2006) 209–209.

[11] K. Dabov, A. Foi, V. Katkovnik, and K. Egiazarian. Image denoising by sparse 3-D transform-domain collaborative filtering. *Image Processing, IEEE Transactions on* 16, (2007) 2080–2095.